Noname manuscript No.
(will be inserted by the editor)

Pixel statistical analysis of diabetic *vs.* non-diabetic foot-sole spectral terahertz reflection images.

G. G. Hernandez-Cardoso[1,2] · **M. Alfaro-Gomez**[3] · **S. C. Rojas-Landeros**[1,2] · **I. Salas-Gutierrez**[4] · **E. Castro-Camus**[1,2]

Received: date / Accepted: date

Abstract In this article we present a series of hydration mapping images of the foot soles of diabetic and non-diabetic subjects measured by terahertz reflectance. In addition to the hydration images we present a series of RYG-color-coded (Red Yellow Green) images where pixels are assigned one of the three colors in order to easily identify areas in risk of ulceration. We also present the statistics of the number of pixels with each color as a potential quantitative indicator for diabetic foot-syndrome deterioration.

Keywords Terahertz imaging · Diabetic foot · Tissue Hydration · Biomedical applications

1 Introduction

Diabetes mellitus is nowadays considered a global pandemic owing to its high prevalence worldwide, affecting ∼8.5% of the world population [1]. It generates extraordinary costs for patients and public health systems across the world. Diabetes occurs when the pancreas does not produce enough insulin or the insulin it produces is not used effectively by the body [2]. Insulin is a hormone that regulates blood sugar levels. Over time, high sugar levels cause severe damage to various organs and systems, especially the nerves and blood vessels

[1]Centro de Investigaciones en Optica, A.C.
Loma del Bosque 115, Lomas del Campestre, Leon, Guanajuato 37150, Mexico.
E-mail: enrique@cio.mx

[2]Laboratorio Nacional de Ciencia y Tecnologia de Terahertz.

[3]Departamento de Matematicas y Fisica, Centro de Ciencias Basicas.
Universidad Autonoma de Aguascalientes
Av. Universidad 940, Ciudad Universitaria, C.P. 20131, Aguascalientes, AGS, Mexico.

[4]Hospital Angeles Leon
Av. Cerro Gordo 311, Lomas del Campestre, 37150 Leon, Guanajuato, Mexico.

[3]. The combination of microvascular and neurological deterioration causes diabetic foot syndrome. A patient with diabetic foot presents dehydration and loss of sensation in his/her lower limbs [4] which, in many cases, leads to the formation of ulcers that can become infected and if not properly and timely treated, result in the amputation of the affected limb [5]. Due to the complexity and prevalence of this condition an early diagnostic test to avoid these consequences is highly desirable.

Terahertz radiation has certain characteristics that allow multiple applications in various areas. Particularly, in medicine [6–8] and biology [9–11] given that the hydration level of biological tissues can be determined non-destructively by terahertz radiation since it is strongly absorbed by water, furthermore, THz photon energy is too low to cause ionization, and therefore, tissue damage. Terahertz has been proposed as a potential tool for the diagnosis of skin burns [12,13] as well as skin [14], breast [15], colon [16,17] and other forms of cancer [18], as well as other health conditions such as corneal deterioration [19].

We recently proposed terahertz imaging as a potential diagnostic tool for the diabetic foot [20]. In that publication the hydration was monitored on the sole of the foot of a control group and a group of diabetic patients. Although significant differences were observed regarding the water content of both groups, it is still necessary to define indicators to perform a better diagnosis of the syndrome, follow up the treatments given to the patients and help in the prevention of injuries. In order to overcome these limitations, we propose a new form of image display that shows the clearly distinguished areas of the foot sole in three different colors depending on the degree of hydration: red for low hydration ($W_{\%}$ <47%), yellow for medium hydration (47%<$W_{\%}$ <58%) and green for good hydration ($W_{\%}$ >58%) which, in turn, indicate the degree of deterioration as *high-*, *medium-* and *low-risk*, respectively.

2 Methods

2.1 Subject selection

The right-foot of a group of 38 diagnosed diabetic patients from the Hospital Regional Leon of the Instituto de Seguridad y Servicios Sociales de los Trabajadores del Estado were imaged with one exception, which was a patient that already had undergone right-foot amputation, in that case the left foot was imaged instead. Of the images taken 26 were discarded because they were unsuitable for analysis, mainly because the patient moved during the data acquisition. In addition 33 volunteers were recruited among students and employees of the Centro de Investigaciones en Optica A.C., none of them was a diagnosed diabetic, however, no control test was applied to this group. Of those images 12 were discarded following the same criteria as for the diabetic patients. This is the same set of measurement presented in our previous article [20].

2.2 Imaging setup

A platform was designed to maintain the patient in a sitting position, while his/her feet rested on a high density polyethylene window. Underneath the window a raster scanning XY platform moved a $\pm 12.5^\circ$ emitter-lens-lens-detector confocal ensemble whose focus lies on the polyethylene window. A point by point terahertz time-domain signal was acquired using a Menlo systems Tera-K-15 spectrometer properly interfaced with the XY platforms. Further details on the setup can be found in [20].

2.3 Signal processing

The pixel-by-pixel hydration was determined by least square fitting of the reflection transfer function

$$H = \frac{|t_{12}(\omega) r_{23}(\eta, \omega) t_{21}(\omega)|}{|r_{12}(\omega)|}, \tag{1}$$

where t_{12} and t_{21} are the air-polyethylene and polyethylene-air transmission Fresnel coefficients, r_{12} and $r_{23}(\eta, \omega)$ are the air-polyethylene and polyethylene-foot reflection Fresnel coefficients, the last one has a dependence on the water volumetric fraction η that will be discussed in the next paragraph. Experimental values for H can be obtained by windowing, in the time domain signal, the first reflection of the air-polyethylene window interface and the polyethylene-foot interface and numerically calculating the ratio of their respective Fourier transform amplitudes.

The LLL effective medium model [21] was used to obtain an analytic expression of the complex permittivity

$$\varepsilon_{\text{mix}}^{1/3} = \eta \varepsilon_{\text{water}}^{1/3} + (1 - \eta) \varepsilon_{\text{dry tissue}}^{1/3}, \tag{2}$$

as a function of the permittivities of water $\varepsilon_{\text{water}}$ [22], dehydrated tissue $\varepsilon_{\text{dry tissue}}$ [20] and the water volumetric fraction η. From this expression the refractive index of the skin can be obtained for any hydration level and from it $r_{23}(\eta, \omega)$. In addition an *ad hoc* empirical correction factor was considered in order to take into account minor alignment errors and other factors present in the experiment that would be hard to incorporate in the equations [23].

2.4 RYG-image construction

The sensitivity and specificity of a diagnostic test are defined as

$$\text{Sens.} = \frac{\text{True positives}}{\text{False negatives} + \text{ True positives}} \tag{3}$$

and

$$\text{Spec.} = \frac{\text{True negatives}}{\text{False positives} + \text{ True negatives}}. \tag{4}$$

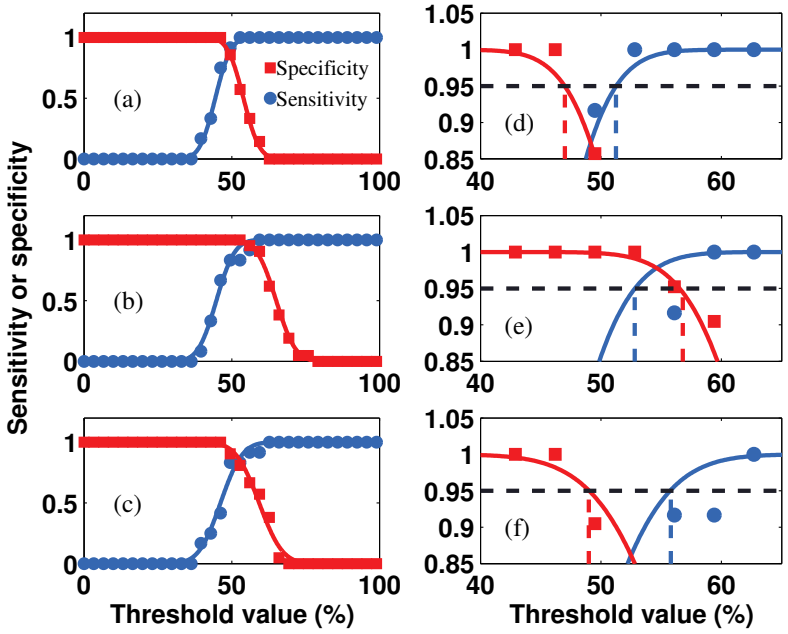

Fig. 1 Sensitivity (blue circles) and specificity (red squares) values for the tests of average humidity across the sole of the foot (a), humidity in the big toe (b) and humidity in the center of the heel (c) with respect to the variation in the threshold (humidity percentage). Zoom in 95% for sensitivity (blue) and specificity (red) in order to define a hydration threshold from the three tests: average humidity (d), humidity in the big toe (e) and humidity in the center of the heel (f).

since we currently do not have a proper golden standard for *early* diabetic foot syndrome, we decided to take as true positives all the diagnosed diabetics, as a first approximation. In order to find the threshold values to consider a test positive we plotted these two quantities as a function of the threshold value used to separate negative and positive outcomes of the test, these plots are shown in Fig. 1(a-c). Since the population shows a normal distribution, and therefore the sensitivity and specificity show an error-function-like behaviour, we fitted such functions to the datasets which are shown in the plots. In order to determine the threshold values that guarantee both a sensitivity and a specificity larger than 0.95 we found the lowest threshold that gives such specificity (47.0% see Fig 1(d)) and the highest threshold that gives that sensitivity (55.8% see Fig 1(f)). The RYG images were constructed in such a way that pixels with water volumetric fractions below 47.0% were colored in red, pixels with water volumetric fractions above 55.8% were colored in green, and pixels with a moisture in between were colored in yellow.

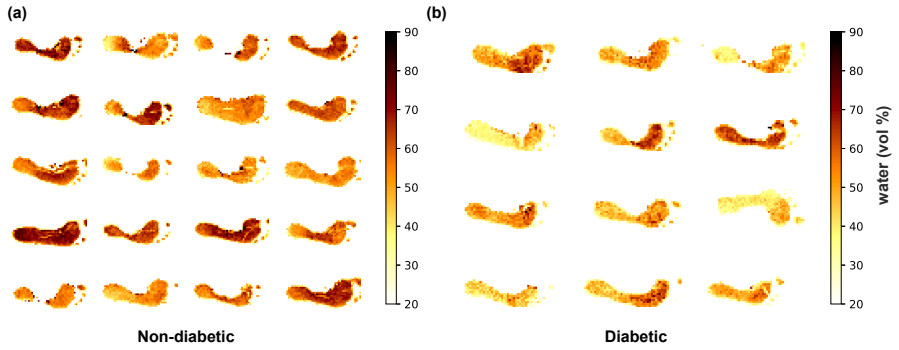

Fig. 2 Water volumetric fraction of the skin measured by terahertz imaging and subsequent processing. The soles of (a) non-diabetic volunteers have a higher water content than the soles of (b) diabetic patients.

3 Results

Terahertz imaging with the appropriate processing, as described in the methods section, allows to quantify the hydration of the skin on the sole of the foot at each measurement point. In Fig 2 two panels, where the processed terahertz spectroscopic images obtained for each of the volunteers are shown, the color map represents the degree of hydration on the sole of each volunteer's foot of the (a) control and (b) diabetic groups. As seen in the figure, the degree of hydration of the control group is higher than the diabetics. Yet, while informative, the hydration maps are relatively hard to interpret, with the exception of extremely dehydrated or extremely well hydrated feet soles. In order to simplify the interpretation of the images, RYG-color-coded images are presented in Fig. 3. In this case the differences between the two groups are far more obvious, furthermore, it is easy to identify that the diabetic patients in Fig. 3(b) [line 2, column 1], [line 3, column 2], [line 3, column 3] and [line 1, column 1] present a proportion of the feet surface with a deterioration larger than the rest of the diabetic group, it is also possible to identify that the patient shown in [line 2, column 3] shows a proportion of the area with good hydration comparable to a non-diabetic. A careful analysis of the RYG-images allows us to observe that almost all diabetics show red areas in their heels and toes, which is consistent with the areas where diabetics commonly develop ulcers, therefore, it is possible to foresee that a scheme similar to this one could have potential in order to predict areas at risk of developing ulcers before they actually appear.

In order to have a more quantitative idea of how the RYG-color scheme separates the control and diabetic groups, we decided to do some statistics of the fraction of pixels that meet each of the three hydration conditions and

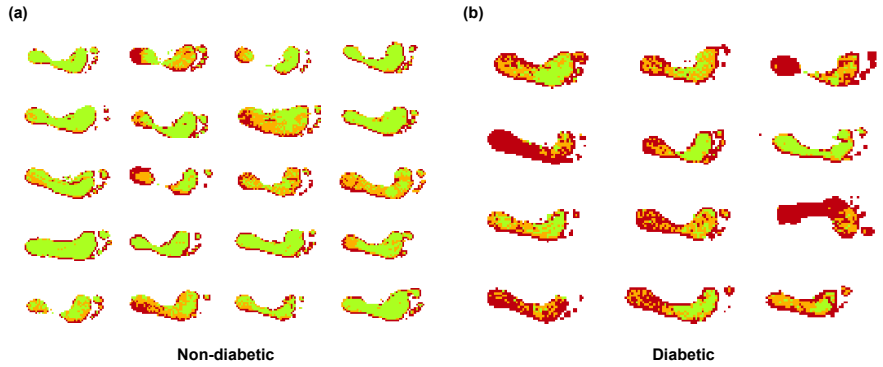

Fig. 3 RYG-images show the foot of (a) non-diabetic subjects and (b) diabetic patients in three different colors: red for hydration below 47%, yellow for hydration between 47% and 55.8% and green for hydration above 55.8%. There is a clear distinction between the two groups. A large proportion of the control group has mostly green pixels with relatively small areas in red, in comparison, almost all diabetics show a relatively small fraction of green pixels, and some of them have very significant fraction of the sole classified as red.

identify if this could provide an additional quantitative indicator to help the diagnostician. The percentage occupied by each of the colors (red, yellow and green) in the sole of the foot of the volunteers, diabetics and non-diabetics, was obtained. The values are shown in the Fig. 4(a-c). While there is a clear difference in the proportion of red and green pixels between the two groups, the fraction of yellow pixels seems to be statistically similar between the two groups. At this point it is worth pointing out that all non-diabetics have under 45% of red pixels, while two thirds of the diabetic subjects have over 45% of red pixels. Analogously, all non-diabetic images have more than 18% of their pixels in green, while over half of the diabetic's images have less than 18% of their pixels classified as green.

An additional indicator of the level of deterioration is the difference of the fraction of green and red pixels which we define as

$$G - R = \%\ Green\ pixels - \%\ Red\ pixels. \tag{5}$$

Such difference is presented in Figure 5 for all subjects of both groups. The plot shows that all non-diabetics have a $G - R$ difference higher than -18%, if we take this as a threshold, 82% of the diabetics show a G-R difference below that.

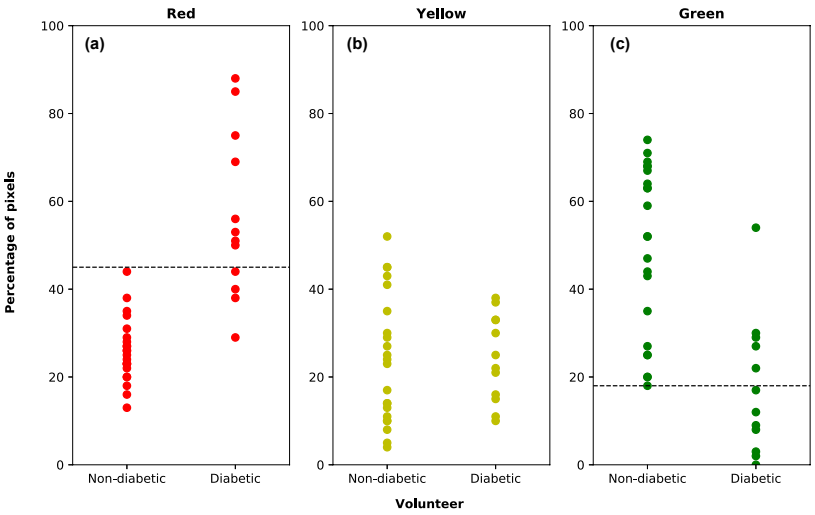

Fig. 4 The percentage of occupation of each color in the sole of the foot of the diabetic and non-diabetic volunteers is shown in each of the three graphs. It can be seen that diabetic patients present, statistically, (a) higher percentage of red pixels and (c) lower percentage of regions of green pixels than non-diabetics. Both groups show similar percentages of (b) yellow pixels.

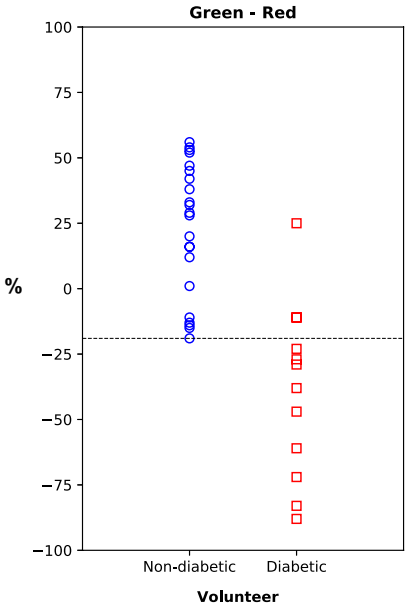

Fig. 5 $G - R$ difference obtained by subtracting the percentage of red pixels from the percentage of green pixels. Non-diabetic subjects (circles) present $G - R$ values between -18% and +65% while diabetic patients (squares) are all below +30% and more than 4/5 of them are below -18%. The dotted line is located along the -18% level to visualize the separation between groups.

4 Conclusions

From the amount of water in different regions of the sole of the foot, quantitative indicators of the degree of deterioration of the skin can be determined and with it the risk of developing an ulcer. The RYG-images allow a better visualization of regions of interest, that is, areas on the sole of the foot with larger risk level. In addition, they help the diagnostician to determine the severity and extent of the diabetic foot problem. The statistics of the number of red, yellow and green pixels in conjunction to the absolute hydration values serve as quantitative measures of the problem and can therefore be used in the evaluation of the patients' evolution and the assessment of new treatments. While very encouraging it is worth mentioning that these results present a few limitations. Firstly, the lack of a golden standard for early diabetic foot deterioration is not incorporated. Secondly, the control group was not screened for diabetes, so there is a possibility that there are a few diabetics within our control group. Thirdly, there is an age difference between the control group, which contains a number of young graduate students, and the diabetic group, which is mostly in the 50 to 65 year band, this could result in a bias of our results. Yet, we consider that our results suggest great potential of the technique and we are working in gaining access to larger control and diabetic groups in order to conduct a more rigorous clinical trial.

5 Measurements on human subjects

The protocol for measurements on human subjects was approved by the Ethics Committee of the Hospital Regional Leon of the Instituto de Seguridad y Servicios Sociales de los Trabajadores del Estado on the 18/SEP/2014. All patients signed an informed consent form.

Acknowledgements The authors would like to acknowledge the financial support of CONACyT through grants 280392, 255114 and 252939 and scholarships 291236 and 290915. We also want to thank H. L. Lopez-Lemus who helped with the logistics of the measurements at ISSSTE-Leon, and the ethics committee paperwork.

References

1. W.H. Organization, *Global status report on noncommunicable diseases* (Geneva, Switzerland, 2014)
2. A.D. Association, Diabetes Care **37**(3), 887 (2014)
3. D.M. Nathan, New England Journal of Medicine **328**, 1676 (1993)
4. H. Pham, D.G. Armstrong, C. Harvey, L.B. Harkless, J.M. Giurini, A. Veves, Diabetes Care **23**(5), 606 (2000)
5. A.J. Boulton, L. Vileikyte, G. Ragnarson-Tennvall, J. Apelqvist, The Lancet **366**(9498), 1719 (2005)
6. K. Shiraga, Y. Ogawa, T. Suzuki, N. Kondo, A. Irisawa, M. Imamura, Journal of Infrared, Millimeter, and Terahertz Waves **35**(5), 493 (2014)
7. E. Pickwell, V.P. Wallace, Journal of Physics D: Applied Physics **39**(17), R301 (2006)

8. Q. Sun, Y. He, K. Liu, S. Fan, E.P.J. Parrott, E. Pickwell-MacPherson, Quantitative Imaging in Medicine and Surgery **7**(3), 345 (2017)
9. S.W. Smye, J.M. Chamberlain, A.J. Fitzgerald, E. Berry, Physics in Medicine and Biology **46**(9), R101 (2001)
10. P.H. Siegel, IEEE Transactions on Microwave Theory and Techniques **52**(10), 2438 (2004)
11. E. Castro-Camus, M. Palomar, A.A. Covarrubias, Scientific Reports **3**, 2910 EP (2013)
12. Z.D. Taylor, R.S. Singh, M.O. Culjat, J.Y. Suen, W.S. Grundfest, H. Lee, E.R. Brown, Opt. Lett. **33**(11), 1258 (2008)
13. P. Tewari, N. Bajwa, R.S. Singh, M.O. Culjat, W.S. Grundgest, Z.D. Taylor, C.P. Kealey, D.B. Bennett, K.S. Barnett, A. Stojadinovic, Journal of Biomedical Optics **17**(4), 040503 (2012)
14. R.M. Woodward, B.E. Cole, V.P. Wallace, R.J. Pye, D.D. Arnone, E.H. Linfield, M. Pepper, Physics in Medicine and Biology **47**(21), 3853 (2002)
15. P.C. Ashworth, E. Pickwell-MacPherson, E. Provenzano, S.E. Pinder, A.D. Purushotham, M. Pepper, V.P. Wallace, Opt. Express **17**(15), 12444 (2009)
16. F. Wahaia, G. Valusis, L.M. Bernardo, A. Almeida, J.A. Moreira, P.C. Lopes, J. Macutkevic, I. Kasalynas, D. Seliuta, R. Adomavicius, R. Henrique, M. Lopes, Journal of Molecular Structure **1006**(1), 77 (2011)
17. L.H. Eadie, C.B. Reid, A.J. Fitzgerald, V.P. Wallace, Expert Systems with Applications **40**(6), 2043 (2013)
18. C. Yu, S. Fan, Y. Sun, E. Pickwell-MacPherson, Quantitative Imaging in Medicine and Surgery **2**(1), 33 (2012)
19. Z.D. Taylor, J. Garritano, S. Sung, N. Bajwa, D.B. Bennett, B. Nowroozi, P. Tewari, J.W. Sayre, J.P. Hubschman, S.X. Deng, E.R. Brown, W.S. Grundfest, IEEE Transactions on Terahertz Science and Technology **5**(2), 184 (2015)
20. G.G. Hernandez-Cardoso, S.C. Rojas-Landeros, M. Alfaro-Gomez, A.I. Hernandez-Serrano, I. Salas-Gutierrez, E. Lemus-Bedolla, A.R. Castillo-Guzman, H.L. Lopez-Lemus, E. Castro-Camus, Scientific Reports **7**, 42124 EP (2017)
21. H. Looyenga, Physica **31**(3), 401 (1965)
22. H.J. Liebe, G.A. Hufford, T. Manabe, International Journal of Infrared and Millimeter Waves **12**(7), 659 (1991)
23. P.U. Jepsen, U. Møller, H. Merbold, Opt. Express **15**(22), 14717 (2007)